

Perturbed hematopoiesis in individuals with germline DNMT3A overgrowth Tatton-Brown-Rahman syndrome

Ayala Tovy,^{1,2} Carina Rosas,^{1,2} Amos S. Gaikwad,³ Geraldo Medrano,³ Linda Zhang,^{1,2,4} Jaime M. Reyes,^{1,2,5} Yung-Hsin Huang,¹ Tatsuhiko Arakawa,^{1,2} Kristen Kurtz,³ Shannon E. Conneely,³ Anna G. Guzman,^{1,2} Rogelio Aguilar,³ Anne Gao,³ Chun-Wei Chen,^{1,2,4} Jean J. Kim,^{1,2,6} Melissa T. Carter,⁷ Amaia Lasa-Aranzasti,⁸ Irene Valenzuela,⁸ Lionel Van Maldergem,⁹ Lorenzo Brunetti,^{3,10} M. John Hicks,¹¹ Andrea N. Marcogliese,³ Margaret A. Goodell^{1,2,3,4,5,6#} and Rachel E. Rau^{1,3#}

¹Stem Cells and Regenerative Medicine Center, Baylor College of Medicine, Houston, TX, USA; ²Department of Molecular and Cellular Biology, Baylor College of Medicine, Houston, TX, USA; ³Department of Pediatrics, Baylor College of Medicine and Texas Children's Hospital, Houston, TX, USA; ⁴Graduate Program in Translational Biology and Molecular Medicine, Baylor College of Medicine, Houston, TX, USA; ⁵Department of Molecular and Human Genetics, Baylor College of Medicine, Houston, TX, USA; ⁶Department of Education, Innovation and Technology, Baylor College of Medicine, Houston, TX, USA; ⁷Department of Genetics, Children's Hospital of Eastern Ontario, Ottawa, Ontario, Canada; ⁸Department of Clinical and Molecular Genetics, Vall d'Hebron University Hospital and Medicine Genetics Group, Vall d'Hebron Research Institute, Barcelona, Spain; ⁹Centre de Génétique Humaine and Integrative and Cognitive Neuroscience Research Unit EA481, University of Franche-Comté, Besançon, France; ¹⁰Department of Medicine and Surgery, University of Perugia, Perugia, Italy and ¹¹Department of Pathology Texas Children's Hospital and Department of Pathology and Immunology, Baylor College of Medicine, Houston, TX, USA

#MAG and RER contributed equally as co-senior authors.

©2022 Ferrata Storti Foundation. This is an open-access paper. doi:10.3324/haematol.2021.278990

Received: April 14, 2021.

Accepted: May 21, 2021.

Pre-published: June 3, 2021.

Correspondence: RACHEL E. RAU - rachel.rau@bcm.edu

MARGARET A. GOODELL - goodell@bcm.edu

SUPPLEMENTAL DATA

Perturbed hematopoiesis in individuals with germline DNMT3A overgrowth Tatton-Brown-Rahman syndrome

Ayala Tovy^{1,2}, Carina Rosas^{1,2}, Amos S. Gaikwad³, Geraldo Medrano³, Linda Zhang^{1,2,4}, Jaime M. Reyes^{1,2,5}, Yung-Hsin Huang¹, Tastuhiko Arakawa^{1,2}, Kristin Kurtz³, Shannon E. Conneely³, Anna G. Guzman^{1,2}, Rogelio Aguilar³, Anne Gao³, Chun-Wei Chen^{1,2,4}, Jean J. Kim^{1,2,6}, Melissa T. Carter⁷, Amaia Lasa-Aranzasti⁸, Irene Valenzuela⁸, Lionel Van Maldergem⁹, Lorenzo Brunetti¹⁰, M. John Hicks¹¹, Andrea N. Marcogliese³, Margaret A. Goodell^{1,2,3,4,5,6*} and Rachel E. Rau^{1,3*}

1. Stem Cells and Regenerative Medicine Center, Baylor College of Medicine, Houston, TX, USA
2. Department of Molecular and Cellular Biology, Baylor College of Medicine, Houston, TX, USA
3. Department of Pediatrics, Baylor College of Medicine and Texas Children's Hospital, Houston, TX, USA.
4. Graduate Program in Translational Biology and Molecular Medicine, Baylor College of Medicine, Houston, TX, USA
5. Department of Molecular and Human Genetics, Baylor College of Medicine, Houston, TX, USA
6. Department of Education, Innovation and Technology, Baylor College of Medicine, Houston, TX, USA
7. Department of Genetics, Children's Hospital of Eastern Ontario, Ottawa, ON, Canada
8. Department of Clinical and Molecular Genetics, Vall d'Hebron University Hospital and Medicine Genetics Group, Vall d'Hebron Research Institute, Barcelona, Spain
9. Centre de Génétique Humaine and Integrative and Cognitive Neuroscience Research Unit EA481, University of Franche-Comté, Besancon, France
10. Department of Medicine and Surgery, University of Perugia, Perugia, Italy
11. Department of Pathology Texas Children's Hospital and Department of Pathology and Immunology, Baylor College of Medicine, Houston, TX

Supplemental Methods:

Mouse hematopoietic progenitor and peripheral blood staining

Peripheral blood was collected into a tube with anti-coagulant dextran solution and following separation of layers, the top layer containing white blood cells was transferred to a collection tube for RBC lysis for 15 minutes. Femurs, tibias, spleens, lymph nodes and identified masses were harvested and made into single cells suspension by manual trituration. Cells were then washed and stained for 15 minutes for the described populations as previously described by our lab (3, 35). All antibodies used were purchased from BD or Biolegend (Supplemental Table S4). Cells were analyzed by flow cytometry (LSRII, Becton Dickinson) with the FACSDiva software (BD Biosciences). A minimum of 10,000 cells was analyzed per sample, and data was visualized using the FlowJo software (FlowJo, LLC). Classification of stem and progenitor cells: for hematopoietic stem cells (HSC) SLAM markers (Lineage negative, cKit positive, Sca-1 positive, Flk2-, CD150 positive, CD48 negative); multipotent progenitor (MPP) cells (Lineage negative, cKit positive, Sca-1 positive, Flk2-CD150 negative, CD48 negative); common lymphoid progenitors (CLPs) (Lineage negative, IL7ra positive, cKit positive, Sca-1 positive); common myeloid progenitors (CMPs) (Lineage negative, IL7ra negative, cKit positive, Sca-1 negative, CD34 positive, CD16/CD32 negative); megakaryocyte-erythrocyte progenitors (MEPs) (Lineage negative, IL7ra negative, cKit positive, Sca-1 negative, CD34 positive, CD16/CD32 negative); and granulocyte-monocyte progenitors (GMPs) (Lineage negative, IL7ra negative, cKit positive, Sca-1 negative, CD34 positive, CD16/CD32 positive). Classification of erythropoiesis: proerythroblasts (proE) were defined as cells with dim TER119 and bright CD71 expression; TER119 positive cells were then plotted by CD71 and forward side (FSC) to define erythroblasts populations including large, immature erythroblasts (EryA) (bright CD71 expression and high FSC), smaller, more mature erythroblasts (EryB) (bright CD71 expression and low FSC), and the most mature, small erythroblast subset (EryC) (CD71 negative and low FSC).

Human peripheral blood staining

Coded peripheral blood (PB) samples were submitted, without patient identifying information, to the CLIA-certified flow cytometry lab of Texas Children's Hospital where the clinically validated leukemia flow cytometry panel and lymphocyte subset flow cytometry panel were performed. In brief, PB specimens were washed twice with wash buffer (Phosphate buffer saline containing 1% fetal bovine serum and 0.1% sodium azide) and resuspended in approximately the same volume. Approximately 100 μ L of the washed PB specimen was stained with the set of antibodies (Supplemental Table S5 and S6) for 15 minutes at room temperature followed by lysis step using 1x red cell lysis buffer per manufacturer's recommendations (BD Biosciences). Wash buffer was added to neutralize the lysis buffer. The cell suspension was centrifuged at x100g and resuspended in 1mL of wash buffer. Sample acquisition was performed using BD FACS Canto flow cytometer. About 20,000 live events

were acquired using BD DIVA software for the leukemia and lymphocyte subset panel. Data analysis was performed using FCS express DeNovo software. White blood cell (WBC) count to calculate the absolute values on analytes was obtained by using the Sysmex XP300 instrument as recommended by the manufacturer (Sysmex Corporation). All cases underwent flow cytometry testing performed using a standard 31- 74 antibody six-color leukemia panel using a BD FACSCanto flow cytometer and BD FACSDiva 7.5 software for data analysis. Interpretation was conducted by a board-certified hematopathologist who was blinded to the sample identity.

Complete blood count

Blood was collected using EDTA coated tubes and Complete blood count (CBC) was done no later than 12 hours from the time of blood draw for mouse samples and no later than 48 hours after blood draw for human samples. Mouse samples were analyzed on the Hematology Analyzer (Bailo, model OV-360), human samples were analyzed on IDEXX ProcyteDX.

Histopathology

Animals were euthanized, and tissues for downstream analysis were fixed in 4% (vol/vol) buffered formalin and embedded in paraffin. Sections were stained with hematoxylin and eosin using standard protocols.

Cytokine enzyme-linked immunosorbent assay

Human or murine plasma was collected, and the following Elisa analyses were done according to the manufacturers' instructions, time of primary antibody was adjusted to overnight at 4°C. For human: IL6 (Abcam, ab178013). For mouse: IL6 (Sigma, RAB0308-1KT).

Supplemental Tables:

Supplemental Table S1: Table of *DNMT3A* variants identified in TBRs

ID	Mutation type	Age (years)	<i>DNMT3A</i> coding sequence variant	<i>DNMT3A</i> variant protein
TBRs1	Frameshift deletion/insertion	10.11	c.2041_2042delATinsG	p.I81Afs*24
TBRs2	Missense	10.3	n\k	p.R635Q
TBRs3	Frameshift duplication	10.10	c.1974_1975dup	p.R659Pfs*47
TBRs4	Missense	5.7	c.1949T>C	p.L650P
TBRs5	Missense	8	c.1004A>G	p.K335R
TBRs6	Frameshift duplication	25.5	c.1867dupT	p.Y623Lfs*7
TBRs7	Missense	6.5	c.1907T>A	p.V636E
TBRs8	Missense	16.2	c.2644C>A	p.R882S
TBRs9	Missense	7.6	c.1669T>G	p.C557G
TBRs10	Stop gain	8.10	n\k	p.Y528*
TBRs11	Missense	18.4	c.2644C>T	p.R882C
TBRs12	Frameshift deletion	21	c.2340_2343del	p.I780Mfs*21
TBRs13	Missense	7.10	c.2654G>A	p.R882H
TBRs14	Missense	23.1	c.2645G>A	p.R882H
TBRs15	Frameshift deletion	14.2	c.993delC	p.F331Lfs*14
TBRs16	Splice variant	17.2	c.2322+1G	
TBRs17	Missense	8.5	c.2707C>G	p.A903P
TBRs18	Splice variant	17.2	c.493-1G>A	
TBRs19	Frameshift deletion	21.6	c.2275delG	p.V759Wfs*20
TBRs20	Missense	n\k	n\k	p.Y735C
TBRs21	Missense	8.5	c.1480T>G	p.C494G
TBRs22	Missense	25.11	n\k	p.S770L
TBRs23	Frameshift deletion/insertion		c.2193delinsAA	p.F731Lfs*3
TBRs24	Missense	22.5	c.928A>T	p.I310F
TBRs25	Missense	5.6	c.544C>T	p.Q182*
TBRs26	Missense	3.2	c.2063G>A	p.R688H
TBRs27	Missense	12.6	c.2726T>C	p.F909R

TBRS28	Deletion	16.11	del(2)(p23.3) minimal 25,263,627-25,518,425 maximal 25,248,245-25,529,211	
TBRS29	Duplication	n/k	c.2684 2712dupTGCCAGTCATCCGCCACCTCTTCGCTCCG	p.L905Cfs*11
TBRS30	Deletion	41.7	Deletion 24,653,863 – 25,574,264	

n/k, not known

Supplemental Table S2: Table of control individuals' clinical information

ID	Sex	Age (years)	Height (cm)	Height percentile	Weight (kg)	Weight percentile	Relation to TBRS individual	Flow Y/N	CBC Y/N
RR03	M	9	n/k	n/k	n/k	n/k	Sibling	Y	N
RR21	M	10*	n/k	n/k	n/k	n/k	Sibling	Y	Y
RR23	M	3.5	94	9	14.2	23	Sibling	Y	Y
RR35	M	3.5	n/k	n/k	n/k	n/k	Sibling	Y	Y
RR39	F	10	150	96	33	51	Sibling	Y	Y
RR41	F	13.3	180	>99	64.2	87	Sibling	Y	Y
RR42	M	13.3	172	96	60	84	Sibling	Y	Y
RR46	F	11.6	147.7	39	38.2	37	Unrelated	Y	N
RR47	M	8.0	158	83	49.6	79.5	Unrelated	Y	Y
RR48	M	12.1	134.5	85	35.6	95	Unrelated	Y	Y
RR49	F	40	173	95	65	30	Unrelated	N	Y

*, approximate; n/k, not known; Flow, flow cytometric analysis of peripheral blood; CBC, complete blood cell count with white blood cell differential; Y, yes; N, no.

Supplemental Table S3: Table of primers and DNA sequence used for generation of DNMT3A p.W577R

Sequence 5'	
Guide RNA sequence	CGCACATGTAGCAGTTCCAG
Single strand DNA	CCCTCTTCAATGGGCTTTCTTCCAGGTGCTTTTGTGTCGAGTG TGTGGATCTCTTGGTGGGGCCAGGAGCTGCTCAGGCAGCCAT TAAGGAAGAtCCgcggAACTGCTACATGTGCGGGCATAAGGGCACCTATGGG
Genotyping primer F	GTGGGAACAACAACACTGCTGC
Genotyping primer F2	AGCTGCATCGTGGGTCCT
Genotyping primer R	GCGTGAGATGACAGCCTAGA

Supplemental Table S4: Flow antibodies used for mouse blood and tissue analyses

Panel	Pacific Blue	APC-Cy7	PE	PE-Cy7	APC	FITC	BV510	BV605	BV650
BM HSC/CMP	CD3 CD4 CD8 CD11B B220 Ly6G	cKIT	CD150	SCA-1	FLT3	CD34	CD48	CD45.2	
BM Progenitors	CD3 CD4 CD8 CD11B B220 Ly6G	cKIT	CD16/32	Cd127	SCA-1	CD34		CD45.2	
Basic Lineage	CD4 CD8 B220			CD11B Ly6G B220	CD45.2				
Myeloid Panel	CD11B	Ly6G	CD115	Ly6C	CX3CR1	CD45.2			CD11C
B-cell Panel	CD23	CD19	CD43	CD27	B220	IgM	IgD		CD24
T-cell Panel	CD3	CD4	CD8		CD45				
Erythroid Panel	TER119	cKIT	CD71			CD41A			

Supplemental Table S5: Leukemia flow cytometry antibody panel for human blood lineage assessment

Tube#	FITC	PE	PerCP-Cy5.5	PE-Cy7	APC	APC-H7
1	CD7	CD2	CD3	CD8	CD4	CD45
2	Lambda	Kappa	CD19	CD10	CD5	CD45
3	CD15	CD42/61	CD34	CD38	CD11b	CD45
4	CD64	CD16+56	CD14	CD13	CD117	CD45
5	CD99	CD58	CD33	CD25	CD52	CD45
6	CD71	GyA	HLA-DR	CD20	CD22	CD45

Supplemental Table S6: Lymphocyte subset flow cytometry antibody panel for human blood T- and B- cell subset analysis

Tube #	FITC	PE	PerCP-Cy5.5	PE-Cy7	APC	APC-H7
1	CD45RA	CD2	CD3	CD25	CD45RO	CD45
2	Lambda	Kappa	CD19	CD10	CD5	CD45
3	CD7	CD16+56	CD3	CD20	CD22	CD45
4	TCR $\alpha\beta$	TCR $\gamma\delta$	CD3	CD8	CD4	CD45

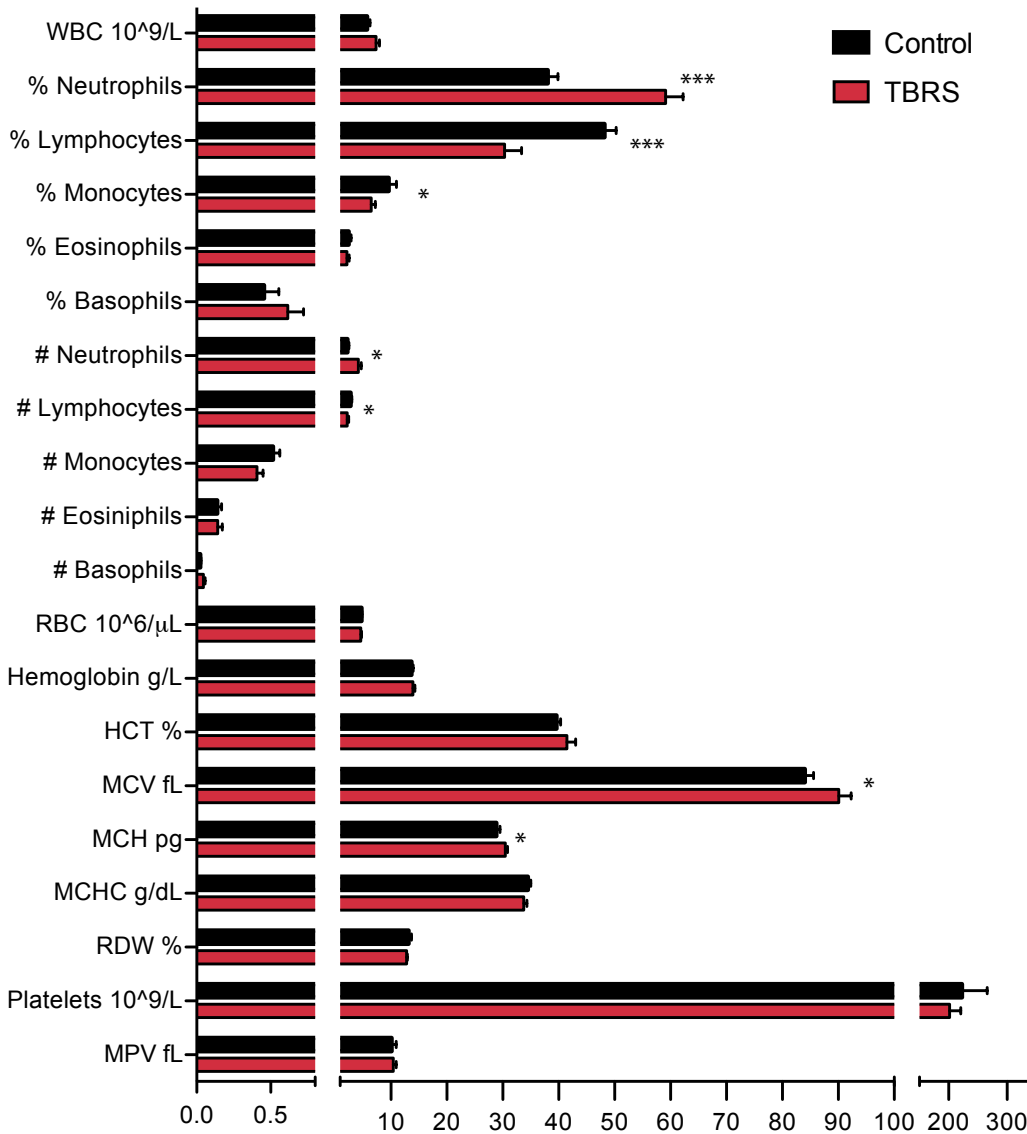
Supplemental Table S7: Pathological characterization of the malignancies identified in HET293 mice

ID	Genotype	Type of malignancy	Features
17	HET293	Lymphoma	B-cell lymphoma involving axillary lymph node (0.59 g)
18	HET293	Lymphoma	B-cell lymphoma involving spleen and liver
21	HET293	Lymphoma	T-cell lymphoma in spleen and liver
40	HET293	Lymphoma	B-cell lymphoma involving BM, liver and spleen; BM also with focal histolytic sarcoma.
		Histiocytic sarcoma	
10	HET293	myeloproliferative neoplasm (MPN)	EMH in the liver; Spleen with marked red pulp expansion, EMH and increased stromal; Flow cytometry of PB, BM, spleen, and liver with >90% myeloid cells
2a	HET293	Angiosarcoma	Tumor adjacent to spleen; Spleen with metastatic angiosarcoma
25	HET293	Angiosarcoma	Metastatic angiosarcoma in spleen; Liver involvement by metastatic histiocytic sarcoma
		Histiocytic sarcoma	
2b	HET293	Acute myeloid leukemia	Leukemic cells infiltrating BM, spleen and liver; Chloromatous mass in abdomen
14	WT	Lymphoma	T-cell lymphoma in spleen and liver

Supplemental Table S8: Differentially methylated regions in LCLs derived from an individual with *DNMT3A*-297deletion (297del) compared to LCLs derived from a sibling of a TBRS individual with WT *DNMT3A*. (Table uploaded as a separate excel file)

Supplemental Figures and Figure Legends

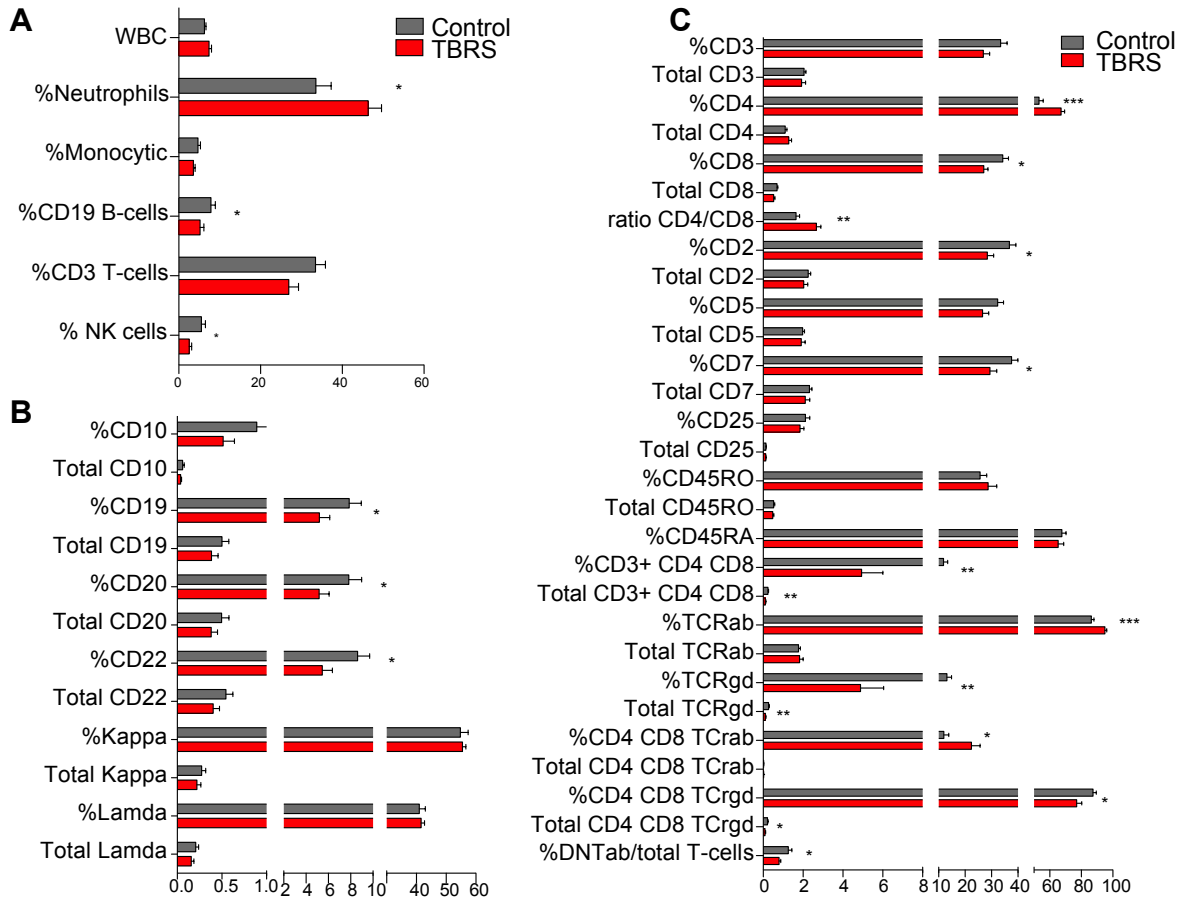
Supplemental Figure S1



Supplemental Figure S1: Summary of complete blood cell count results for TBRS and control

individuals. Average of all CBC parameters comparing TBRS (n=13) to control (n=9) individuals. Bars represent sample means; error bars represent standard error. WBC, white blood cell count; RBC, red blood cell count; HCT, hematocrit; MCV, mean corpuscular volume; MCH, mean corpuscular hemoglobin; MCHC, mean corpuscular hemoglobin concentration; RDW, red blood cell distribution width; MPV, mean platelet volume; %, percentage of each cell type; #, absolute number of each cell type; *, p<0.05; ** p<0.01; ***, p<0.001.

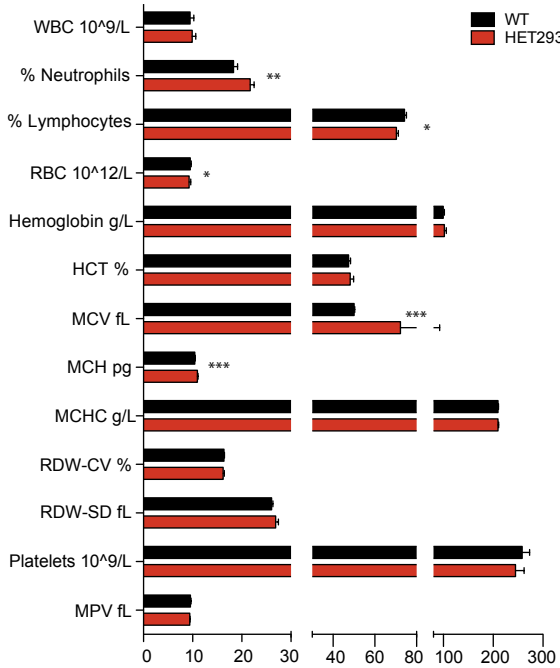
Supplemental Figure S2



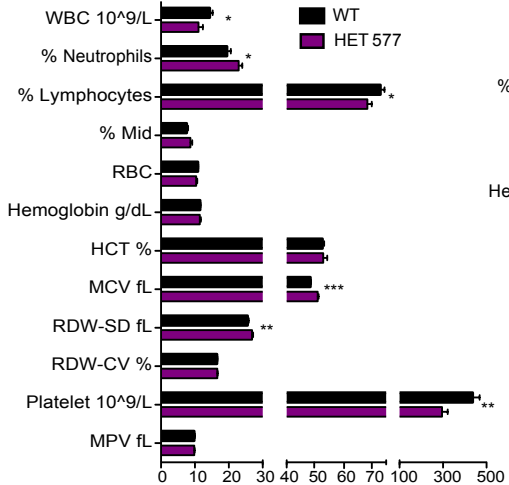
Supplemental Figure S2: Summary of flow cytometry findings from blood of TBRS and control individuals. Average of all the analyzed markers in peripheral blood comparing TBRS (n=15) to control (n=10) individuals. Bars represent sample means; error bars represent standard error. DNT, double negative T-cells; *, p<0.05; ** p<0.01; ***, p<0.001.

Supplemental Figure S3

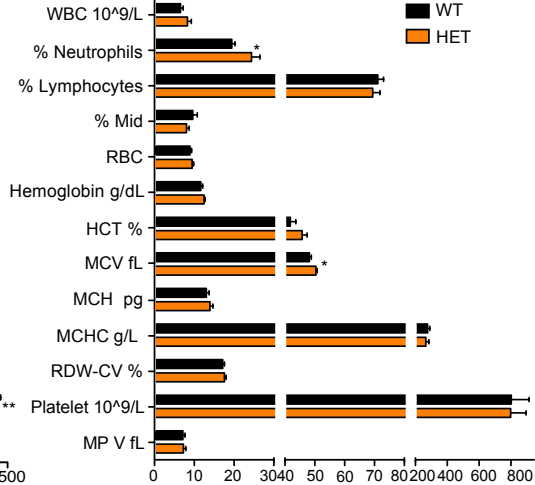
A



B



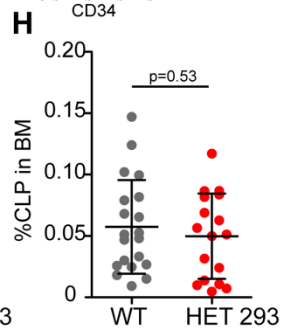
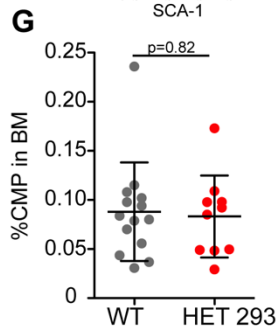
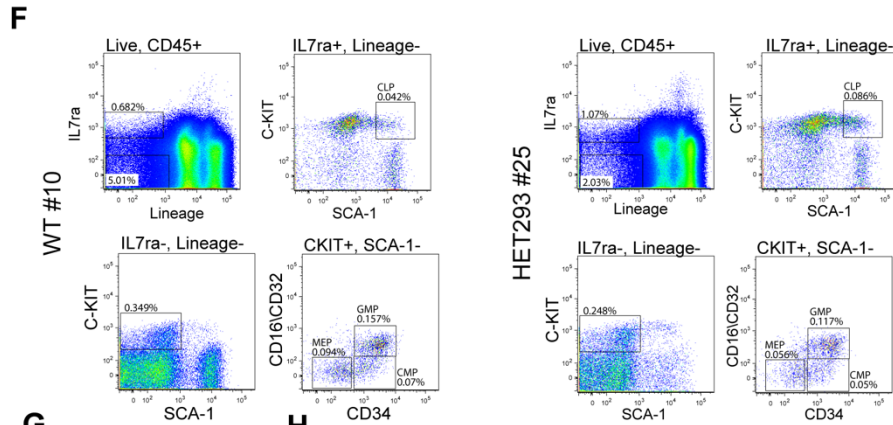
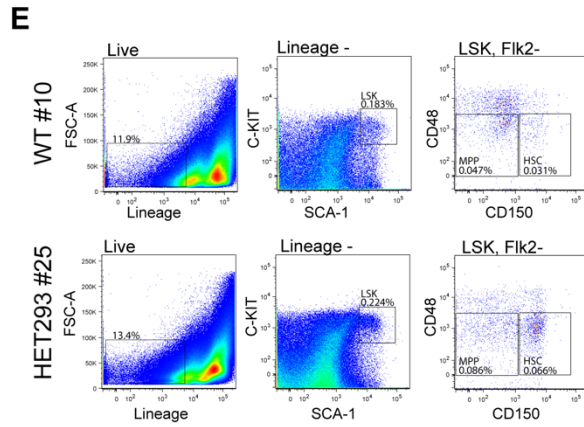
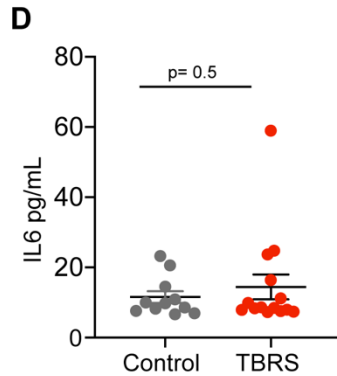
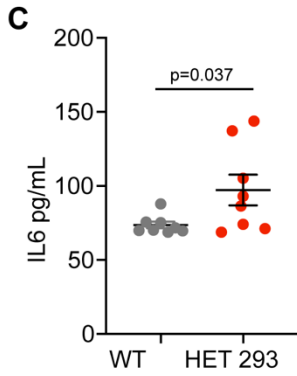
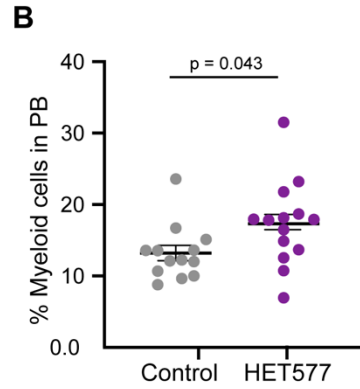
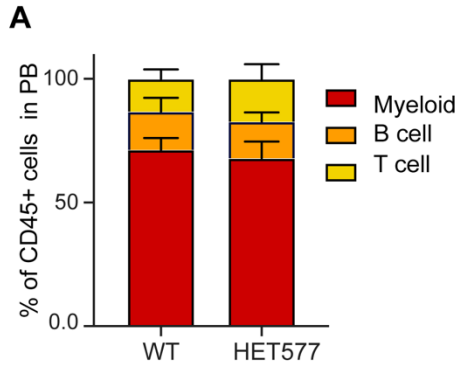
C



Supplemental Figure S3: Summary of complete blood cell count results from *Dnmt3a* mutant and WT mice. Average of all CBC parameters comparing A) HET293 mice (n=23) and WT littermate controls (n=31) B) HET577 mice (n= 17) and WT littermates (n=19), and C) HET mice (n=10) and WT littermates (n=10). Bars represent sample means; error bars represent standard deviation. WBC, white blood cell count; RBC, red blood cell count; HCT, hematocrit; MCV, mean corpuscular volume; MCH, mean corpuscular hemoglobin; MCHC, mean corpuscular hemoglobin concentration (not available for HET577 cohort); RDW, red blood cell distribution width; MPV, mean platelet volume; Mid, combined value of blood cells other than neutrophils and lymphocytes; *, p<0.05; ** p<0.01; ***, p<0.001.

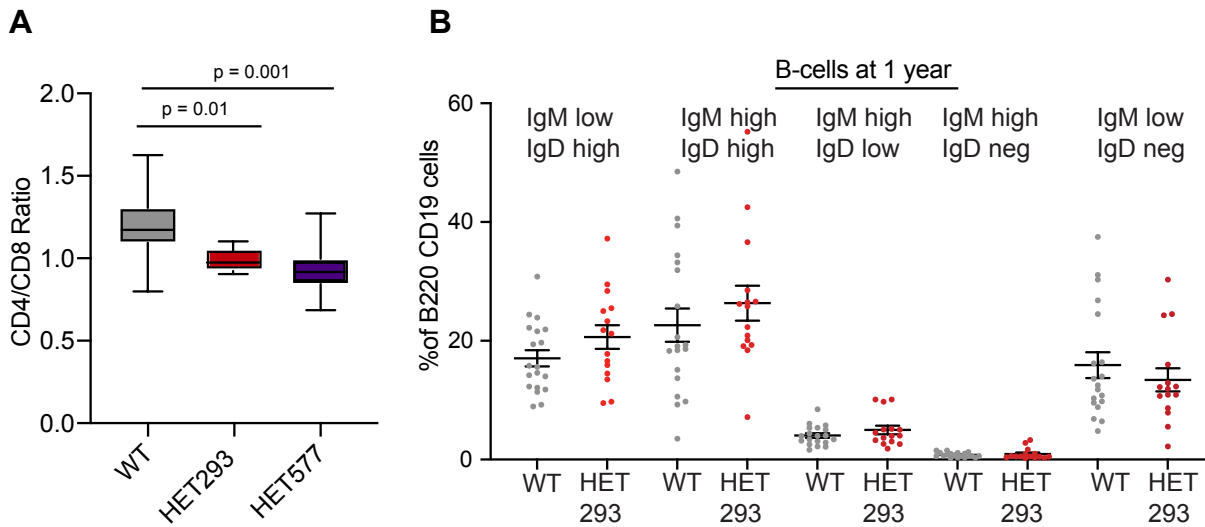
WBC, white blood cell count; RBC, red blood cell count; HCT, hematocrit; MCV, mean corpuscular volume; MCH, mean corpuscular hemoglobin; MCHC, mean corpuscular hemoglobin concentration (not available for HET577 cohort); RDW, red blood cell distribution width; MPV, mean platelet volume; Mid, combined value of blood cells other than neutrophils and lymphocytes; *, p<0.05; ** p<0.01; ***, p<0.001.

Supplemental Figure S4



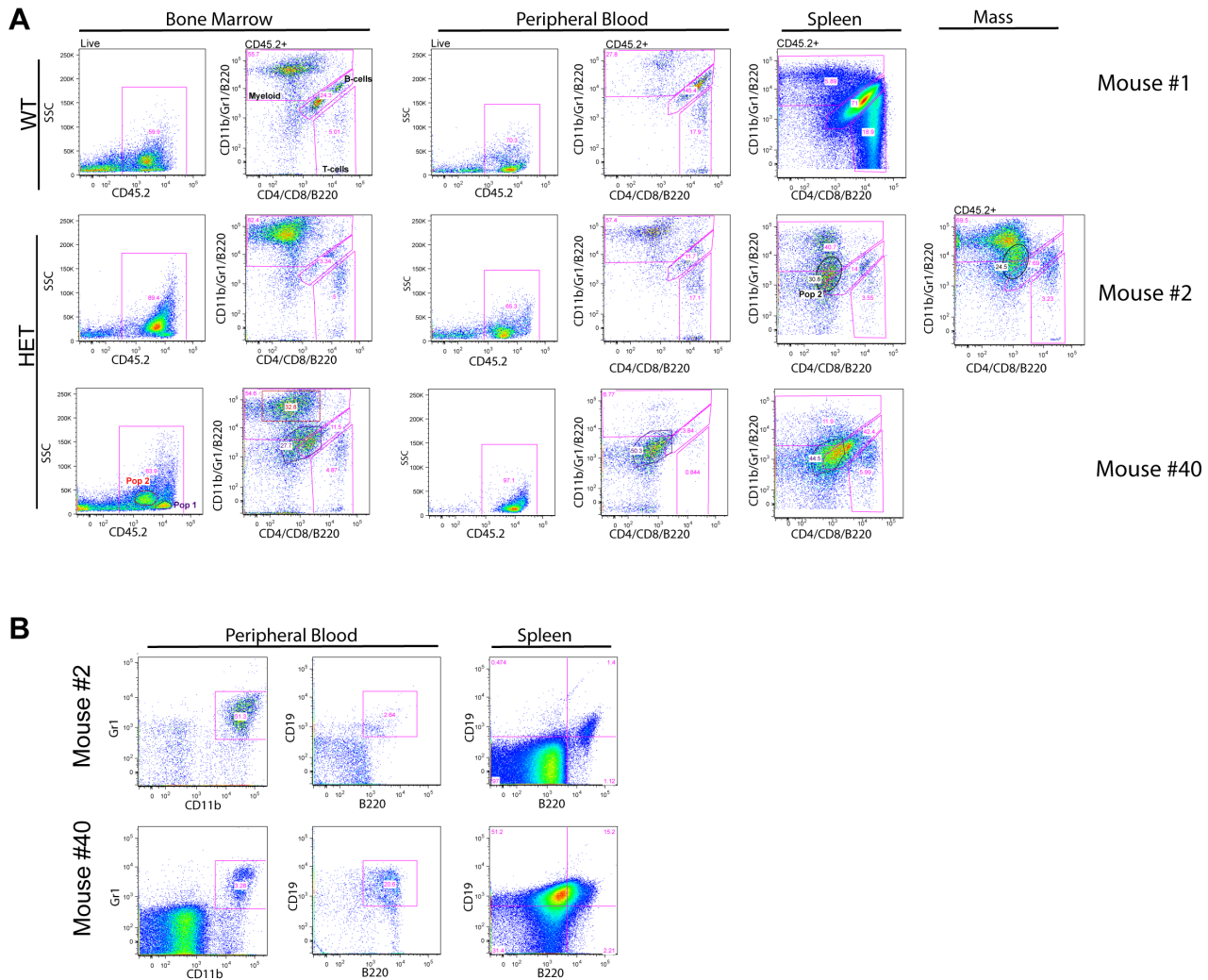
Supplemental Figure S4: Myeloid expansion associated with upregulation of pro-inflammatory cytokines. Flow cytometric analysis of bone marrow CD45+ leukocytes depicting A) relative distribution of myeloid, T- and B-cells in the HET577 (n=14) mice compared to WT (n=12). B) Quantification of the percentage of myeloid cells in the bone marrow of HET577 mice and WT mice as determined by flow cytometry. C) ELISA based measurement of IL6 levels in the plasma of 1-year old HET293 (n=8) compared to WT (n=8) mice. D) ELISA based measurement of IL6 levels in the plasma of TBRS individuals (n=16) compared to controls (n= 11). Mouse bone marrow flow cytometry assessment of E) hematopoietic stem cells (HSCs), multipotent progenitors (MPPs), F) common myeloid progenitor cells (CMPs), common lymphoid progenitors (CLP), megakaryocyte-erythrocyte progenitors (MEPs), and granulocyte-monocyte progenitors (GMPs). G) Quantification of CMPs in HET293 (n=10) and WT (n=14) mice, and H) CLPs in HET293 (n=17) and WT (n=20) mice.

Supplemental Figure S5



Supplemental Figure S5: Flow cytometric analysis of peripheral blood lymphocytes in *Dnmt3a* mutant mice. Analysis of T-cell subtypes including A) CD4+/CD8+ ratio from total CD3+ T-cells in WT (n=15), HET293 (n=8) and HET577(n=12) mice. B) Distribution of B-cells based on surface expression of IgM and IgD from total B-cells (B220+, CD19+, CD45+ viable cells) comparing WT (n=19) and HET293 (n=15) mice.

Supplemental Figure S6

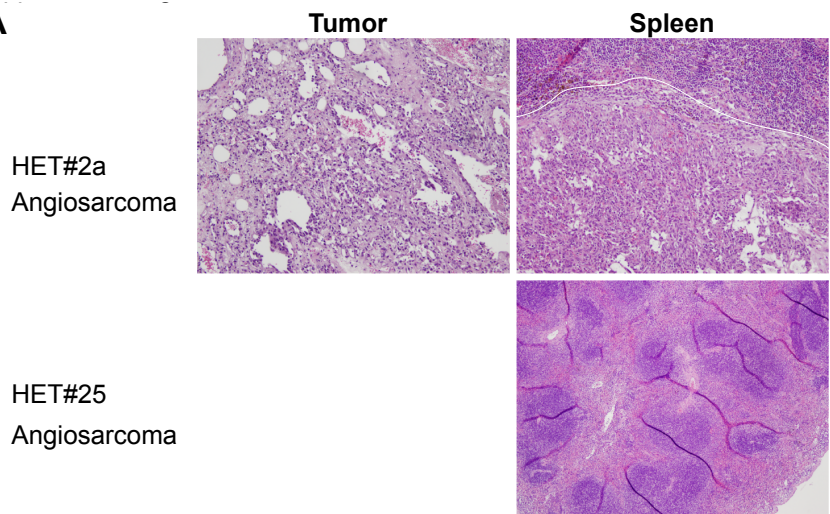


Supplemental Figure S6: Flow cytometric analyses of mice with hematologic malignancies. Flow cytometric analysis was performed on cells isolated from the bone marrow, peripheral blood and spleens in HET293 mice and matched tissue from littermate control WT mice. Shown are representative plots of WT and HET293 mice. A) After first gating on CD45.2+ live cells, lineage analysis was performed, defining cells as myeloid (CD11b/Gr1+), T-lymphoid (CD4/CD8+) or B-lymphoid (B220+). Row one shows results from a healthy WT mouse (Mouse #1). Row two shows a HET293 mouse (Mouse #2) with acute myeloid leukemia including a chloroma in the abdomen. This mouse had a typical CD11b/Gr1 bright population as well as a population with dim expression of myeloid markers (Pop 2, black circle) detected in the spleen and chloroma. Row three shows results from a HET293 mouse (Mouse #40) with a B-cell lymphoma characterized by dim B220 expression (Pop 1, purple outline) with infiltration of the BM and the spleen as well as a myeloid population (Pop 2, red outline) that based on morphology may represent histiocytic sarcoma. B) More detailed analysis of the malignant populations for Mouse #2 (top row) showing the that malignant cells were

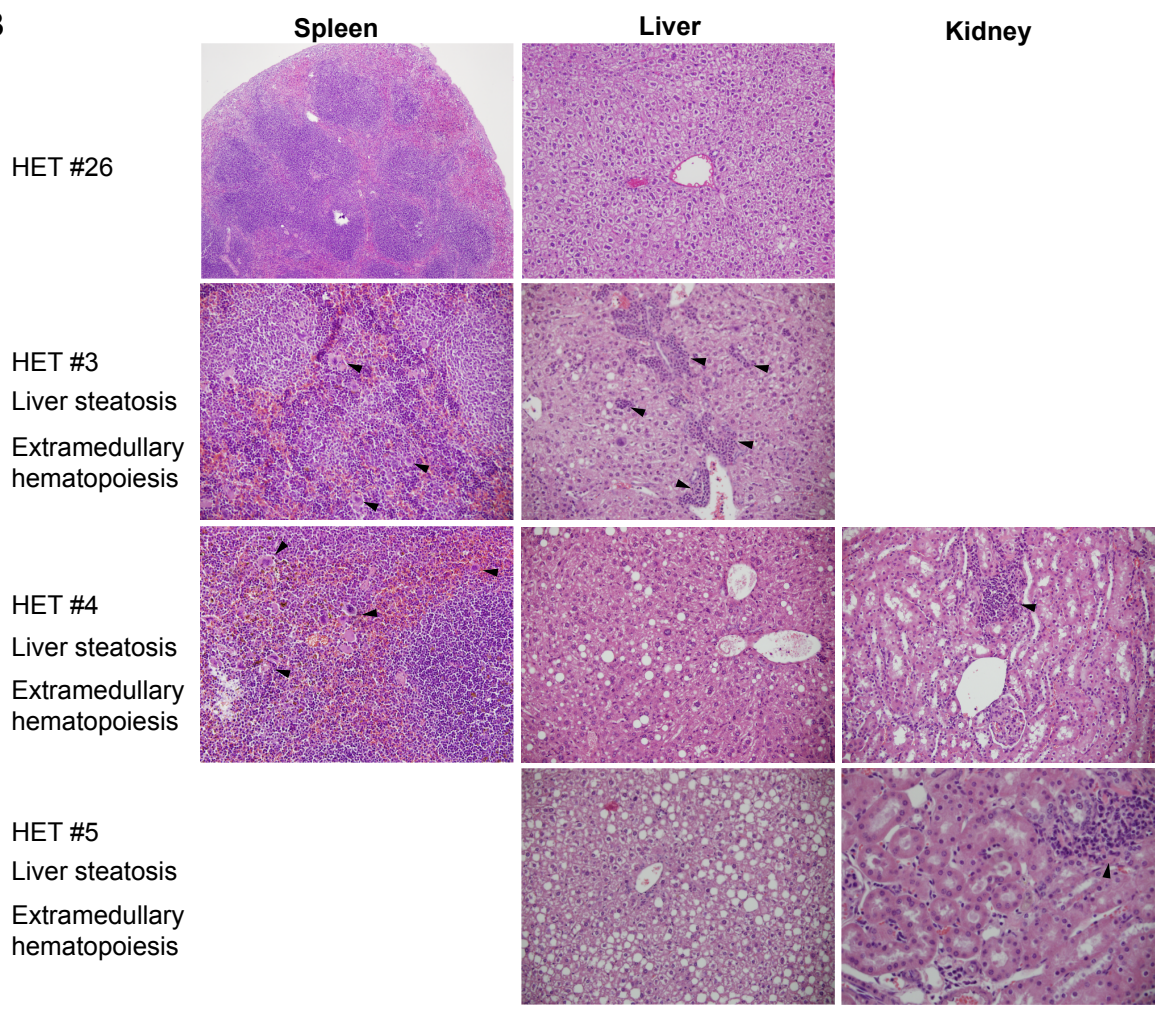
predominantly Gr1+/CD11b+ myeloid cells with a paucity of B220/CD19+ B-cells in the blood and spleen. The malignancy of Mouse #40 (bottom row) is predominantly a B-cell population with variable CD19 and B220 expression.

Supplemental Figure S7

A



B



Supplemental Figure S7: Non-hematological malignancies and non-malignant pathologic findings in HET293 mice. A) Pathologic images of two moribund HET293 mice (HET293 #2a and HET293 #25) with angiosarcomas. For mouse #2a a primary tumor adjacent to the spleen was identified (Tumor). Both mice have involvement of the spleen (for mouse #2, area below the white line marks tumor and for mouse #25 vascular-like invasions into the spleen parenchyma are prominent). B) Pathologic examinations of tissues from HET293 mice without obvious malignancies were also performed. Normal spleen and liver from HET293 Mouse #26 (top row). A subset of HET293 mice had extramedullary hematopoiesis of the spleen, liver and kidneys (arrowheads). Liver steatosis was also noted in a subset of HET293 mice (mild in #3 and 4, extensive in #5).